

A Revisit of the 1946 Aleutian earthquake tsunami



M. Jakir Hossen¹, Leonardo Ramirez-Guzmán² and Anne F. Sheehan¹

1) University of Colorado Boulder, 2) UNAM National Autonomous University of Mexico



University of Colorado
Boulder

Introduction

On April 1, 1946 (163.19°W, 53.32°N; 12:29 UTC) an earthquake with conventional (surface wave) magnitude $M_s=7.4$ (later revised to $M_w=8.6$ by Lopez and Okal, 2006) occurred offshore the Aleutian islands south of Unimak Island. The rise of water was 42 m in the Aleutian Islands (Unimak Island) and 17 m on the Hawaiian Islands (Island of Hawaii). The tsunami arrived without warning and killed 159 people in Hawaii.

Johnson and Satake (1997) (Figure 1) modeled the 1946 tsunami and found good fits to far-field tide gauge records using a shallow dipping underthrust. However, Fryer et al. (2004) and von Huene et al. (2014) (Figure 2) suggested that an earthquake-triggered submarine landslide contributed to the destruction. Based upon bathymetry and marine seismic reflection, von Huene et al. (2016) (Figure 3) suggested that splay fault uplift that elevates the outer mid-slope terrace may have contributed to the tsunami.

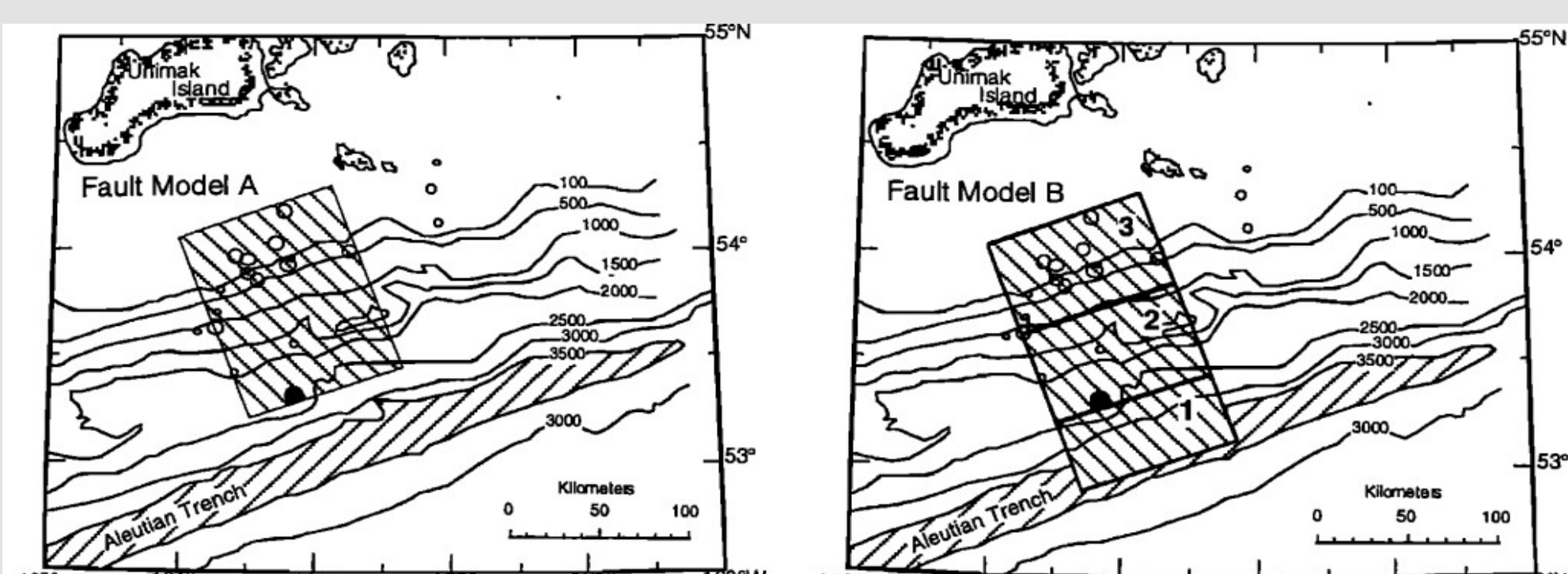


Figure 1: Johnson and Satake, 1997

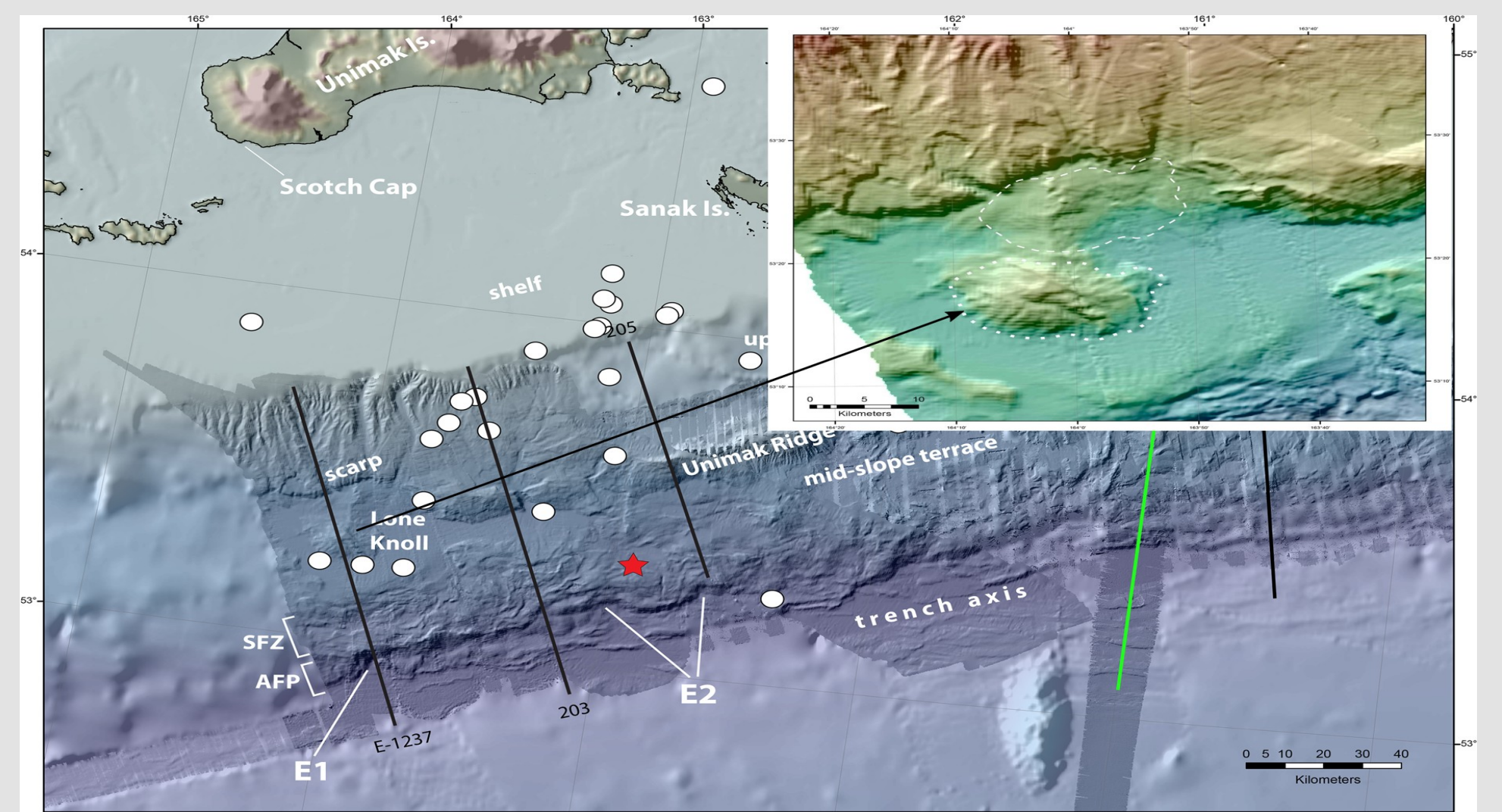


Figure 2: adapted from von Huene et al., 2016 and inset figure from von Huene et al., 2014

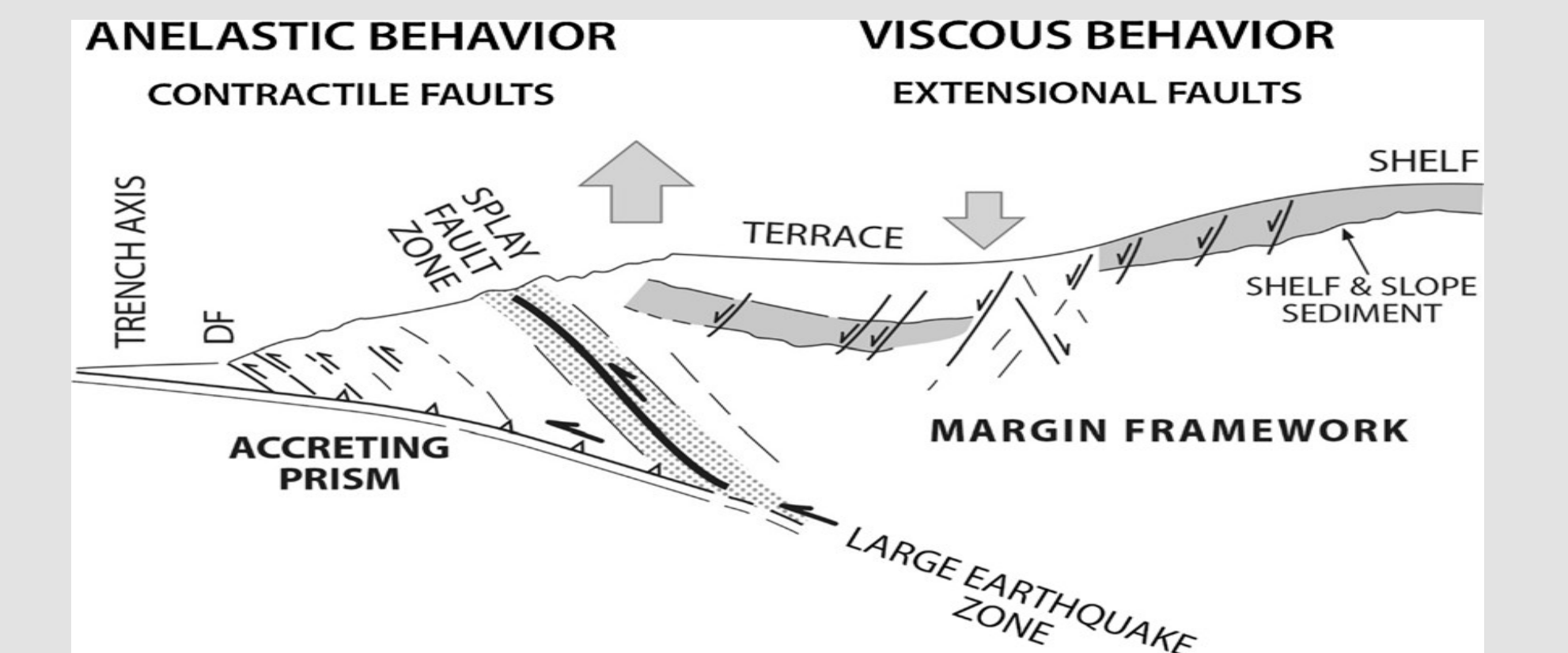


Figure 3: adapted from von Huene et al. (2016)

Data

We considered data from 12 tide gauge stations that recorded the 1946 tsunami. The tide gauges are located at far-field distances in Japan, the US mainland and Hawaii (Figure 4). The tide gauge records are obtained from the National Oceanic and Atmospheric Administration (NOAA) website as well as digitized from the marigram of Green (Transactions, AGU, 1946). In addition to the tide gauge records we estimated synthetic records using tsunami runup data (Figure 6).

Methodology

- We carried out numerical experiments using three different source models: Seismic (suggested by Johnson and Satake, 1997), landslide (proposed by Watts, 1998) and their combination.

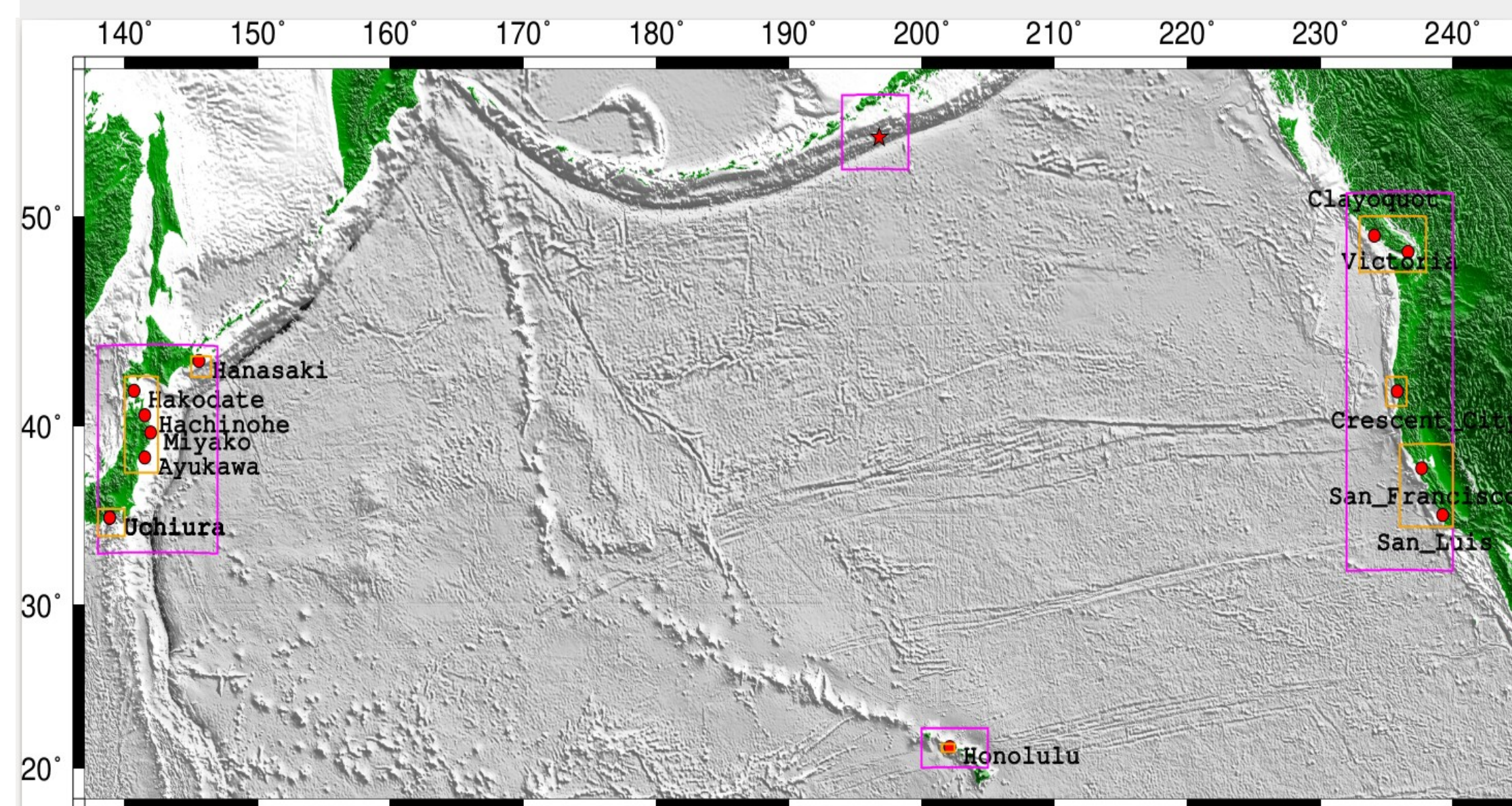


Figure 4: tide gauge stations (red circle), epicenter (red star), outer domain resolution 90 arc sec and inner domain resolutions: 30 sec by magenta boxes and 10 sec by yellow boxes

- We created synthetic observation at real and virtual locations by running seismic, landslide, and combined source models. We also computed Green's functions (GFs) at real and virtual locations by using JAGURS (Baba et al., 2015) parallelized tsunami propagation model that solves the nonlinear Boussinesq dispersive equations in spherical coordinates using a finite difference scheme.

- We next applied Green's Function based Time Reverse Imaging (GFTRI) method (Hossen et al., 2015) for reconstructing the source related to seismic slip, submarine mass failure and their combination.

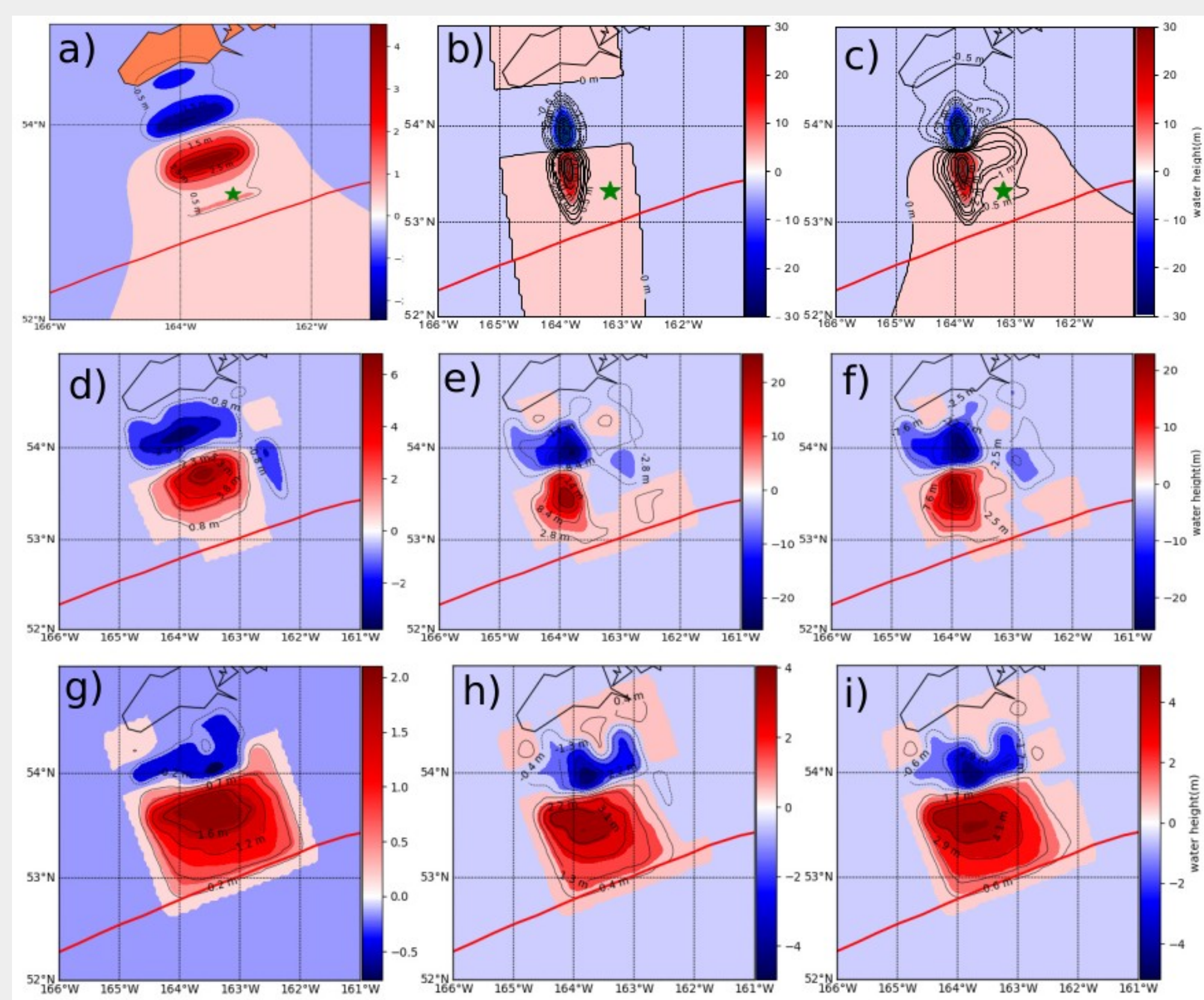


Figure 5 (synthetic tests): Top row shows the sea surface displacement for three different reference models: a) seismic, b) landslide and c) combination of seismic slip and landslide. Second row (d,e,f) shows the recovered sources using both near- and far-field (synthetic) observations and third row (g, h, i) shows the sources recovered only by far-field (synthetic) data.

- Our synthetic tests show that source details are not recovered when using only far-field stations. Both near- and far-field stations are necessary to resolve tsunami source details.

Source estimate using synthetic Observation from runup data:

To create the synthetic tsunami waveform at virtual locations (red triangles) we used runup data collected by Okal et al. (2003). We used Green's (1838) law modified by Baba et al. (2004)

$$H_c = 2H_0h_0^{1/4}$$

where H_0 and h_0 are water height and water depth at runup height location; H_c at virtual locations.

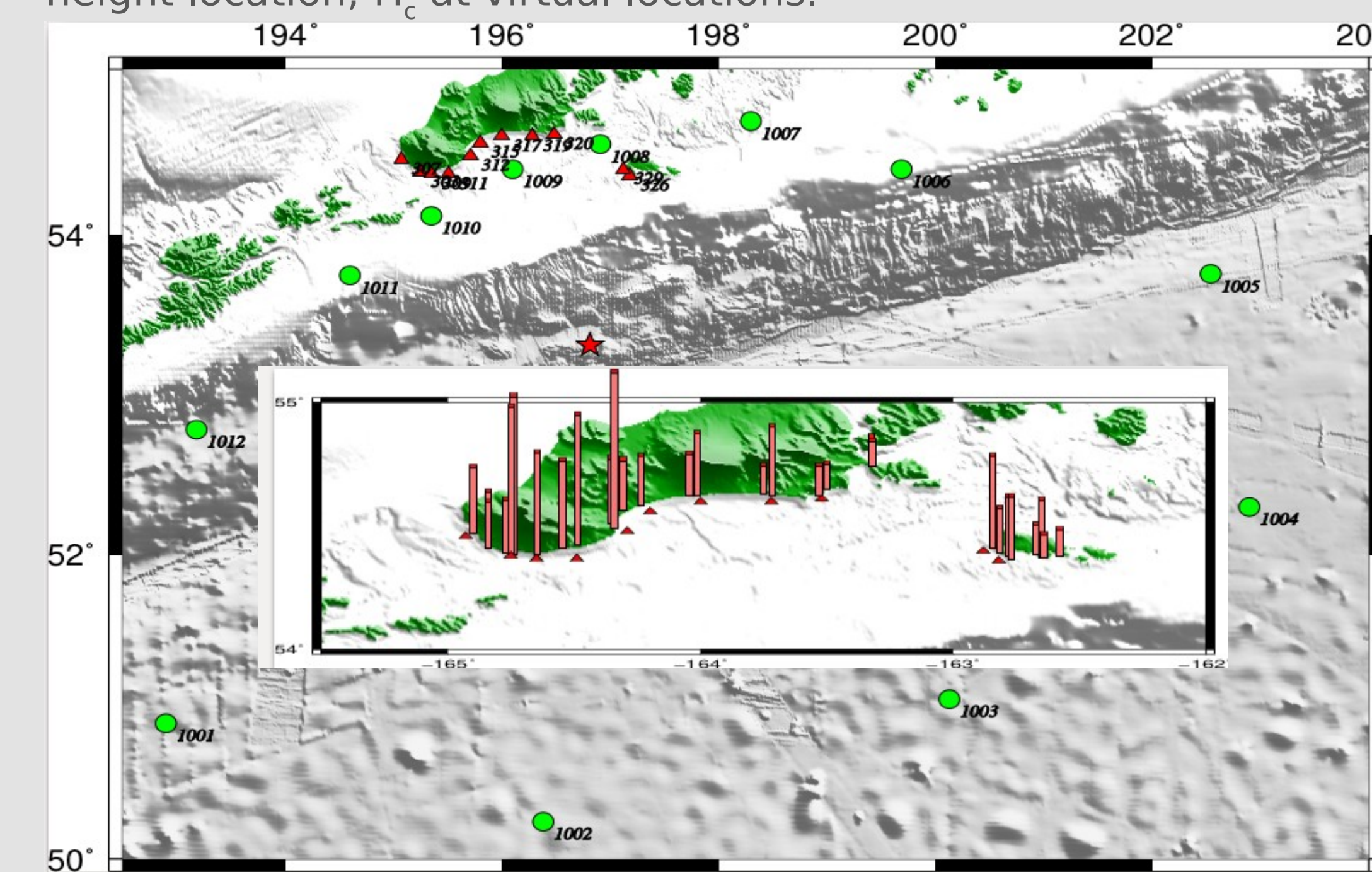


Figure 6: Virtual observation locations surrounding the 1946 earthquake epicenter. Waveforms at green circles are used for recovering reference source models; waveforms at red triangles are used with real observations to estimate a source associated with the 1946 event. Synthetic observations at red triangles are created by adding GFs from four neighboring source grids and then scaling them by run-up height (red bar in the inset). Maximum runup height is 42 m.

Result:

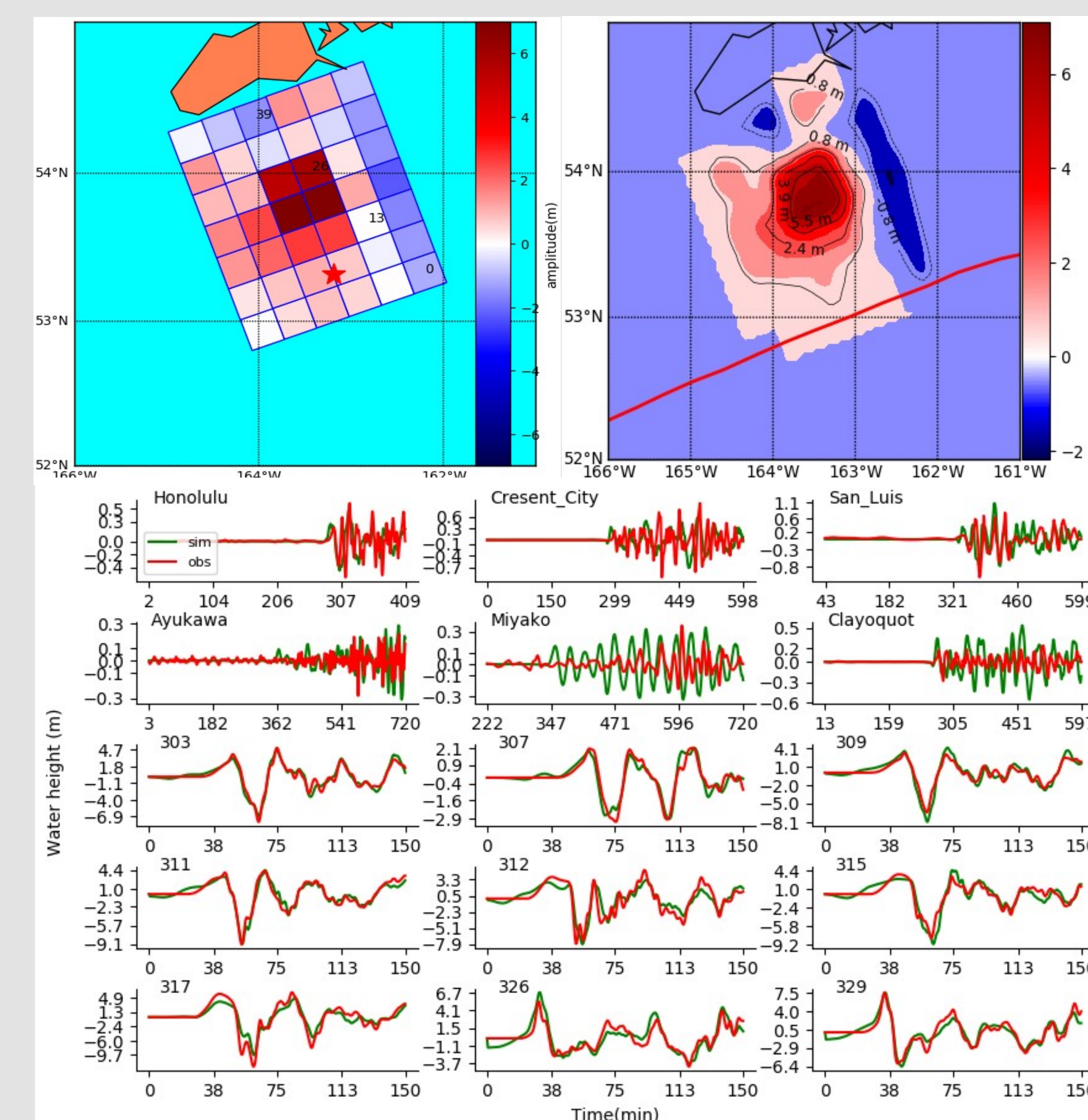


Figure 7: (Upper left) amplitude of unit sources estimated by the synthetic waveforms from run-up height (near-field) and real tide gauge (far-field) data; (upper right) corresponding tsunami sea surface displacement. (Lower panels) shows comparison between observed and computed waveforms. Top six stations are actual tide gauge measurements (Ayukawa, Miyako, Clayoquot, Honolulu, Crescent City, San Luis), remaining stations are virtual observations (as described in Figure 6)

Conclusion

- We conducted numerical experiments to simulate the 1946 Aleutian tsunami using synthetic observations at near field and inversion of both near- (synthetic) and far-field (observed) data.
- Our results show that with only far field data details of the source cannot be recovered. We conclude that both near- and far-field data are essential for recovering the true model.
- Since near-field waveforms are not available for the 1946 event, we developed a new technique to produce synthetic observations at near-field virtual locations using run-up height data.
- Using far-field real tide gauge data and near-field synthetic data we estimated the sea surface displacement which is mostly concentrated in the regions where submarine landslide and splay thrust faulting is suggested to have occurred. Thus, we anticipate that in addition to shallow thrust faulting, the tsunami had a component of either submarine landslide or splay thrust faulting as suggested by von Huene et al. (2014, 2016).

References

- López, A.M. and Okal, E.A., 2006. A seismological reassessment of the source of the 1946 Aleutian tsunami earthquake. *Geophys J Int*, 165(3), pp.835-849.
- Johnson, J.M. and Satake, K., 1997. Estimation of seismic moment and slip distribution of the April 1, 1946, Aleutian tsunami earthquake. *JGR: Solid Earth*, 102(B6), pp.11765-11774
- Fryer, G.J., Watts, P. and Pratson, L.F., 2004. Source of the great tsunami of 1 April 1946: a landslide in the upper Aleutian forearc. *Marine Geology*, 203(3-4), pp.201-218.
- von Huene, R., Kirby, S., Miller, J. and Dartnell, P., 2014. The destructive 1946 Unimak near-field tsunami: New evidence for a submarine slide source from reprocessed marine geophysical data. *Geop. Res. Letters*, 41(19), pp.6811-6818.
- von Huene, R., Miller, J.J., Klaeschen, D. and Dartnell, P., 2016. A possible source mechanism of the 1946 Unimak Alaska far-field tsunami: uplift of the mid-slope terrace above a splay fault zone. In *Global Tsunami Science: Past and Future, Volume I* (pp. 4189-4201). Birkhäuser, Cham.
- Green, C.K., 1946. Seismic sea wave of April 1, 1946, as recorded on tide gages. *Eos, Transactions American Geophysical Union*, 27(4), pp.490-500
- Hossen, M.J., Cummins, P.R., Dettmer, J. and Baba, T., 2015. Time reverse imaging for far-field tsunami forecasting: 2011 Tohoku earthquake case study. *Geop. Res. Letters*, 42(22), pp.9906-9915.
- Watts, P., 1998. Wavemaker curves for tsunamis generated by underwater landslides. *Journal of waterway, port, coastal, and ocean engineering*, 124(3), pp.127-137
- Okal, E.A., Plafker, G., Synolakis, C.E. and Borrero, J.C., 2003. Near-field survey of the 1946 Aleutian tsunami on Unimak and Sanak Islands. *BSSA*, 93(3), pp.1226-1234.
- Baba, T., Takahashi, N., Kaneda, Y., Ando, K., Matsuoka, D. and Kato, T., 2015. Parallel implementation of dispersive tsunami wave modeling with a nesting algorithm for the 2011 Tohoku tsunami. *Pure and Applied Geophysics*, 172(12), pp.3455-3472.
- Baba, T., Hirata, K. and Kaneda, Y., 2004. Tsunami magnitudes determined from ocean-bottom pressure gauge data around Japan. *Geophysical research letters*, 31(8)

Contact:

Email: md.hossen@colorado.edu.